Lizunov et al. http://www.jcb.org/cgi/doi/10.1083/jcb.200412069

Detection of GLUT4 release to the PM by immunofluorescence

Upon insulin stimulation the cells became immunostained with anti-HA antibodies known not to enter the intact PM (Dawson et al., 2001). The HA-tagged exofacial domain of GLUT4 originally exposes to the GLUT4 vesicle lumen and only becomes accessible to the antibodies in the extracellular media if the GLUT4 vesicles fuse with the PM. Accordingly, and consistent with the earlier observations (Malide et al., 1997; Dawson et al., 2001), when the cells were incubated with insulin for 5–15 min at 37°C degree before immunostaining, HA immunofluorescence (Fig. S2 A, red) became highly colocalized with GFP fluorescence of GLUT4 (Fig. S2 A). In contrast, when the cells were first pretreated for 10 min with 100 nM wortmannin, which is known to inhibit insulin signaling, GFP fluorescence showed a punctate pattern with no colocalization with anti-HA immunofluorescence (Fig. S2 B).

FRAP measurements of GLUT-GFP lateral mobility in the PM

Bleaching of GLUT-GFP confined in the TIRF area was performed by turning laser power to the maximum (70 mW). Radius of the circular area of the cell subjected to TIRF depended on the level of squeezing of each particular cell between the coverslips, and varied from 10 to 30 μm. More than 80% of initial fluorescence was bleached out in 3 s. After that, laser power was set to the minimum of level (6 mW) and, with the shutter opening every 15 s, snapshots of TIRF area were acquired for 5–10 min. Stacks of images were further transferred to ImageJ and processed as described below. Mean gray value of the circular ROI representing bleached TIRF area of the cell was calculated for each image and plotted versus time. The experimental data was fitted with a theoretical curve (Axelrod et al., 1976; Soumpasis, 1983; Klein et al., 2003) using the least square algorithm in Maple software (Maplesoft): $F(t) = F_0 + (F_\infty - F_0)e^{(-2\tau/t)}[I_0(2\tau/t) + I_1(2\tau/t)]$, where t is the time, τ is the fitting parameter, F_0 is the fluorescence intensity of the bleached area immediately after bleaching; F_∞ is the fluorescence intensity of the bleached area after recovery to the constant level. I_0 and I_1 are modified Bessel functions. Characteristic time τ obtained from fitting procedure was used to calculate lateral diffusion coefficient for GLUT-GFP from the formula: $D = R^2/4\tau$, where R is the radius of the bleached area.

Kinetic analysis of GLUT4 recycling in primary adipose cells

In adipose cells, GLUT4 cycles between the following main locations (Holman et al., 1994; Lee et al., 1999; Bryant et al., 2002): (a) GLUT4 vesicles (constituting the GLUT4-releasable pool); (b) the rest of subcellular GLUT4 that is not directly delivered to the PM upon insulin stimulation (mainly "endosomal" GLUT4); and (c) GLUT4 associated with the PM, i.e., GLUT4 exposed to the extracellular medium and thus accessible for antibody labeling. The basal distribution of GLUT4 among these three general pools is highly dependent on the experimental system under consideration. In freshly prepared isolated rat adipose cells, most of the GLUT4 is found in the GLUT4 vesicles and little in either the "endosomal" pool or PM; in 3T3-L1 adipocytes, intracellular GLUT4 is roughly divided between the GLUT4 vesicles and the "endosomal" pool, with little in PM; and as reported here and previously (Malide et al., 1997), in primary rat adipose cells cultured for increasing periods, the distribution shifts with culture duration from that observed in the freshly prepared cells to one quite similar to that observed in the 3T3-L1 adipocytes. As noted in the text, we have performed the present TIRFM studies under conditions such that the basal GLUT4 distribution approximates that in freshly prepared cells despite requiring culture times sufficient to provide adequate HA-GLUT4-GFP expression for visualization.

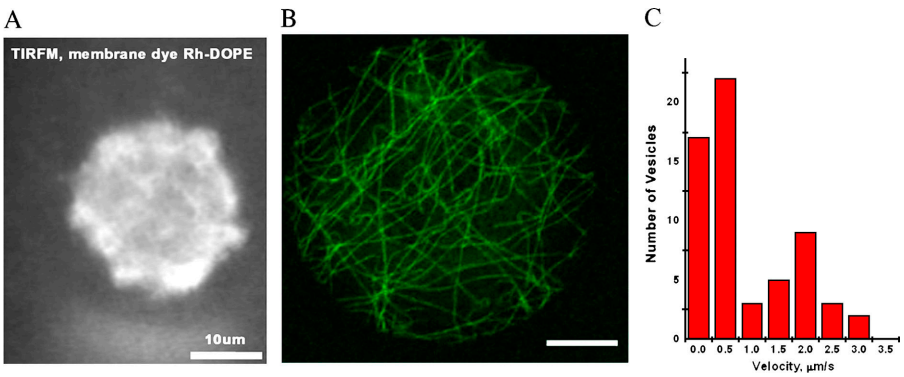

Figure S1. **TIRF-zone geometry, microtubular network and vesicle velocity distribution in adipose cells in the basal state.** (A) TIRFM image of the PM in the TIRF-zone labeled with lipid fluorescent probe phosphatidylethanolamine-lissamine rhodamine B; the entire region of the PM in the TIRF-zone is visible under TIRFM. (B) Cells transfected with GFP-tubulin show an extensive microtubular network that covers the entire cytoplasm. Thin confocal sections were taken every 200 nm through the flattened bottom region of the cell (the same that was used for TIRFM) and then were three-dimensionally reconstructed to visualize the complete microtubular network within the monitored region. Note that many microtubules are sufficiently long (>10 μm) to account for the fast liner movements of the GLUT4 vesicles. (C) Distribution of GLUT4 vesicle velocity, estimated from linear displacements of vesicles recorded on TIRFM time-lapse videos. Note that the distribution exhibits two peaks: 0.6 and 2 μm/s. Bars, 10 μm.

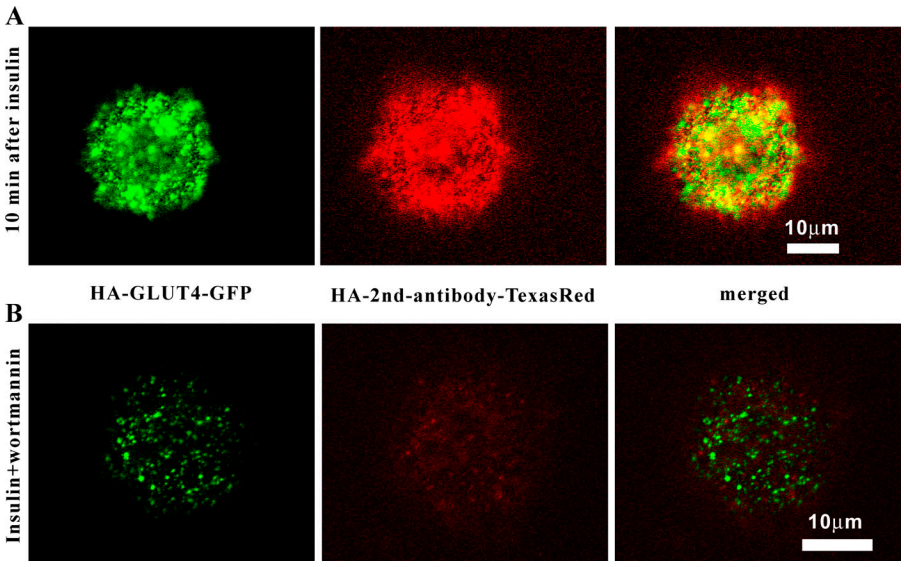

Figure S2. **Immunostaining of HA-GLUT4-GFP on the PM of insulin-stimulated adipose cells and effect of wortmannin.** (A) Cells were incubated with 67 nM insulin for 10 min at 37°C and fixed without permeabilization of the plasma membrane. Cells show high membrane staining with anti-HA antibody visualized with second antibody Texas red. Note high colocalization of immunofluorescence (red) with GFP fluorescence (green). (B) Cells treated with wortmannin and incubated with insulin at the same conditions. Note low immunofluorescence staining and punctate pattern of GLUT4-GFP fluorescence resembling the basal state distribution (as in Fig. 1 C).

A 3-pool model is the minimal one describing the behavior of GLUT4 in rat adipose cells (Holman et al., 1994); moreover, the steady-state distribution of GLUT4 between the three pools described above is consistent with morphological observations (Malide et al., 1997). We extend this model to account for GLUT4 mobility; thus, subdividing GLUT4 vesicles into moving and stationary pools. The vesicle is considered moving if it makes a detectable path (see Fig. 1, A and C). The scheme of this 4-pool model is presented in Fig. S4 A. The following GLUT4 pools are considered: (1) pool 1, GLUT4 in vesicles moving in the TIRF zone; (2) pool 2, GLUT4 in vesicles that remain static in the TIRF zone; (3) pool 3, GLUT4 in the PM or in vesicles fused with the PM so that the GLUT4 is fully exposed to the extracellular medium and accessible to extracellular antibodies; (4) pool 4, the rest of subcellular GLUT4.

As GLUT4 vesicles are uniformly distributed near the PM (see Fig. 1), we assume that the number of GLUT4 vesicles (both moving and stationary) in the TIRF zone is directly proportional to the total number of GLUT4 vesicles in a cell. The same holds for the PM GLUT4. Thus, the dynamics of the fraction of the GLUT4 visible in the TIRF zone correctly represents the overall dynamics of the GLUT4 in the whole adipose cell. Accordingly, we consider the behavior of a fraction of GLUT4, C, corresponding to a single TIRF zone. This fraction is distributed between the four pools described above so that $C1 + C2 + C3 + C4 = C$ and C remains constant. For simplicity, we assume that $C = 1$. The system of equations describing GLUT4 dynamics is as follows (System 1):

$$\cdot C1(t) = -k1C1 + k2C2 + k5C$$

$$\cdot C2(t) = -(k2 + k3)C2 + k1C$$

$$\frac{}{t} C3(t) = -k4C3 + k3C$$

$$\frac{}{t} C4(t) = -k5C4 + k4C$$

$$C1 + C2 + C3 + C4 =$$

The steady-state distribution of GLUT4 is determined from a system of three algebraic equations (System 2):

$$C1C1 + k2C2 + (1 - C1 - C2 - C3)k5 =$$

$$(k2 + k3)C2 + k1C1 =$$

$$\cdot k4C3 + k3C2 =$$

Basal steady-state

From the literature, we know that ~5% of GLUT4 is in the PM (i.e., $C3 = 0.05$) and that the endocytosis rate constant $k4 = 0.06$ min^{-1} (Holman et al., 1994, Malide et al., 2000); from our data, we obtain $C1/C2$, $k1$, and $k2$ (see Table S1). The 3 remaining unknowns, $-k3$, $k5$, and $C1$, are defined by solving the System 2 equations.

Table S1. **The parameters of the kinetic model and steady-state distrbution of GLUT4**

	Basal	Stimulated
$k1$[a]	1/15	1/5
$k2$	1/150	1/150
$k3$	1/15000	1/600
$k4$	10^{-3}	10^{-3}
$k5$	10^{-2}	10^{-2}
$C1$ (GLUT4 moving)	0.08	0.01
$C2$ (GLUT4 stationary)	0.85	0.34
$C3$ (PM)	0.05	0.58
$C4$(subcellular rest)	0.02	0.07

$k1$ is estimated from the mean distance <l> the vesicle passes before getting tethered for the first time: $k1 \sim <V>/<l>$, where <V> is the mean vesicle velocity (approximated as 1 μm/s from Fig. S3), and <l> = 15 (15 ± 6) μm in the basal state and 5 (5 ± 2) μm in the insulin-stimulated state, respectively (see Fig. 3 D). $k2$ in the basal state is estimated from the ratio of mobile/stationaty vesicles: $k2 = k1^{a}(C2/C1)$ provided that $k3$ is significantly smaller than $k2$; $C2/C1$ obtained experimentally is ~10 ($C2/C1 = (N_{total} - N_{moving})/N_{moving} \sim 14/1.4$ where N_{total} is the number of GLUT4 vesicles detected in a ROI of 100 μm^2 randomly selected in a snapshot of the TIRF zone and N_{moving} is the number of moving vesicles in a ROI of the same area (the numbers were averaged over 20 different cells). We note that while at each moment many vesicles are stationary, in the basal state the attachment to the PM is mostly reversible: vesicles will continue moving until they reach the fusion site on the PM as each GLUT4 molecule ultimately cycles through the PM. $C1$ and $C2$: in the basal state, more than 90% of GLUT4 is sequestered subcellularly and this GLUT4 fails to colocalize with endosomal markers (Malide et al., 1997) indicating that it is all sequestered in specialized GLUT4 vesicles; correspondingly, we detected no colocalization of GLUT4 and FM4-64 taken up by adipose cells in the basal state (unpublished data).

[a]Rate constants are s^{-1}.

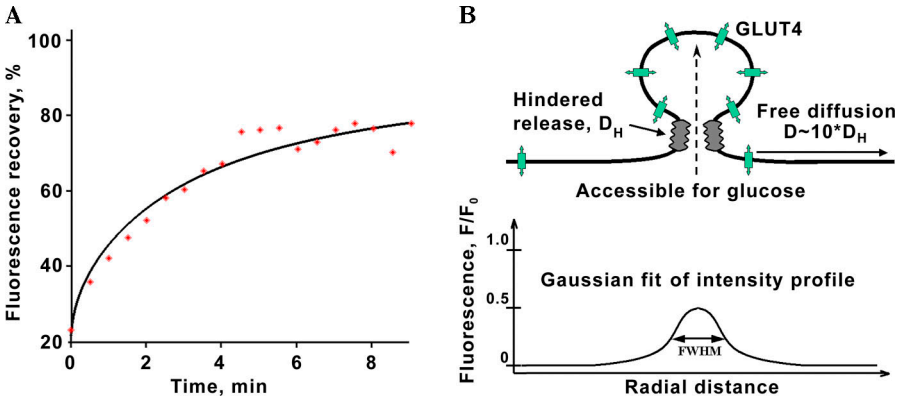

Figure S3. **GLUT4 lateral diffusion estimated by FRAP and by release from fusing vesicles in adipose cells.** (A) GLUT4-GFP fluorescence recovery (red) in a circular region of the PM (10 μm radius), bleached ~15 min after insulin stimulation. Black curve represents theoretical fit with characteristic time of recovery τ = 180 s, giving an estimate of GLUT4 diffusion coefficient: D = 0.14 $\mu m^2/s$. (B) Cartoon illustrating the constrained release of GLUT4 from fusing GLUT4 vesicles. The 10-fold difference of the average observed time of GLUT4 release from the expected time of free diffusion can be accounted by fusion pore constrains (D_H, the rate-limiting diffusion of GLUT4 molecules through the fusion pore). Bottom panel shows lack of widening of the fluorescence profile of a fusing vesicle if diffusion through the pore is significantly slower than diffusion in the plasma membrane.

Insulin steady state

From the literature, we know that ~50% of GLUT4 is translocated to the PM (*C3*) and ~30% remain in GLUT4 vesicles (*C*1 + *C*2) and that *k*4 remains equal to 0.06 min^{-1} (Holman et al., 1994, Malide et al., 2000); from our data, we measure changes in *k*1 (see Table S1). So the unknowns are *k*2, *k*3, *k*5, and *C*1 (or *C*2). They cannot all be determined from the System 2 equations, so we assume that *k*5 remains unchanged and find approximate steady-state values for the remaining unknowns. To verify the assumption, we fit the kinetics of the increase of PM GLUT4 (and the respective reduction of vesicular GLUT4, see Fig. S4, B and C) upon insulin stimulation (solving the System 1 equations using the matrix exponent method) and find that the kinetics are indeed well described assuming that only *k*1 and *k*3 are changed by insulin. If *k*3 is assumed to remain unchanged, the model does not describe either the kinetics of the insulin response or the steady-state distribution of GLUT4 in the insulin-stimulated state.

Conclusion

We conclude that insulin primarily increases the probability of tethering and also stimulates priming of vesicles tethered to specific fusion sites on the PM. This conclusion is well supported by biochemical kinetic data obtained using rat adipose cells.

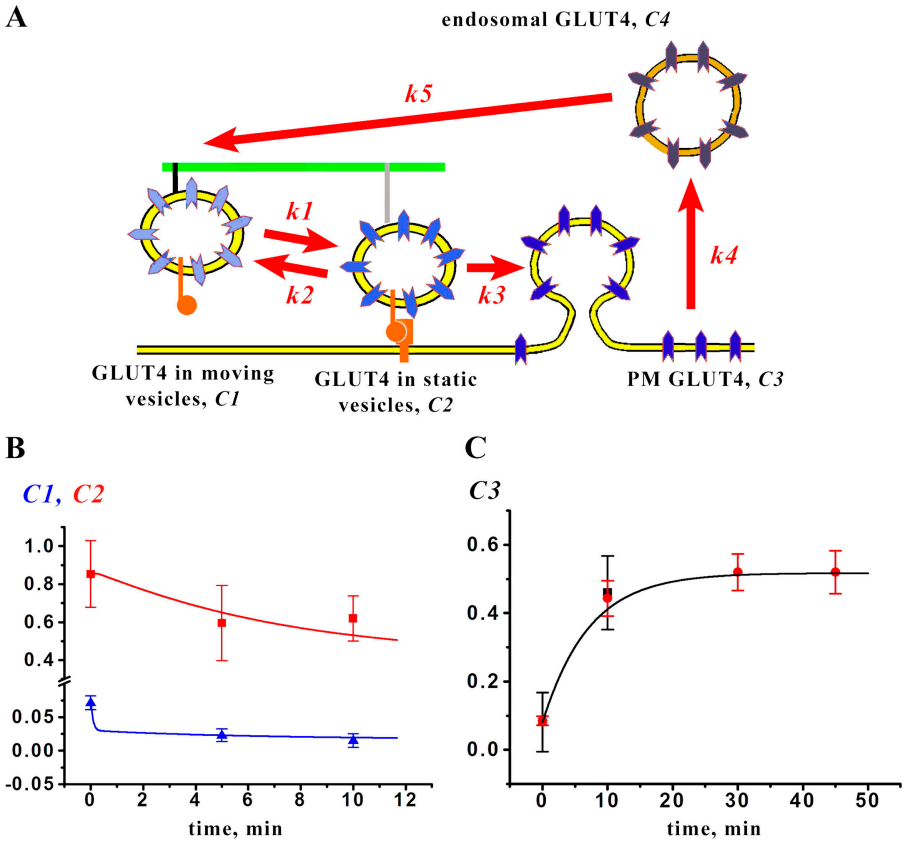

Figure S4. **Model of GLUT4 recycling in primary adipose cells.** (A) Scheme illustrating GLUT4 recycling in a 4-pool model. (B) Changes in the number of moving (blue) and static (red) GLUT4 vesicles upon insulin stimulation. Experimental data are shown by symbols with error bars (the number of vesicles was normalized to correspond to the fraction of GLUT4 vesicles in each corresponding pool); the curves were generated by the model shown in A, taking the basal initial values of *C*1 and *C*2, and assuming that at *t* = 0 and *k*1 and *k*3 instantaneously change to their values characteristic for the insulin-stimulated state. (C) Changes in PM GLUT4 upon insulin stimulation. Experimental data are shown by symbols with error bars; changes are shown in total fluorescence of the TIRF zone corresponding to fusing GLUT4 vesicles (black) and the kinetics of the antibody labeling of PM GLUT4 (red, taken from Dawson et al. [2001]). The initial basal values of C3 and the instantaneous change of *k*1 and *k*3 in response to insulin are assumed as in B.

References

Axelrod, D., D.E. Koppel, J. Schlessinger, E. Elson, and W.W. Webb. 1976. Mobility measurement by analysis of fluorescence photobleaching recovery kinetics. *Biophys. J.* 16:1055–1069.

Bryant, N.J., R. Govers, and D.E. James. 2002. Regulated transport of the glucose transporter GLUT4. *Nat. Rev. Mol. Cell Biol.* 3:267–277.

Dawson, K., A. Aviles-Hernandez, S.W. Cushman, and D. Malide. 2001. Insulin-regulated trafficking of dual-labeled glucose transporter 4 in primary rat adipose cells. *Biochem. Biophys. Res. Commun.* 287:445–454.

Holman, G.D., L. Lo Leggio, and S.W. Cushman. 1994. Insulin-stimulated GLUT4 glucose transporter recycling. A problem in membrane protein subcellular trafficking through multiple pools. *J. Biol. Chem.* 269:17516–17524.

Klein, C., T. Pillot, J. Chambaz, and B. Drouet. 2003. Determination of plasma membrane fluidity with a fluorescent analogue of sphingomyelin by FRAP measurement using a standard confocal microscope. *Brain Res. Brain Res. Protoc.* 11:46–51.

Lee, W., J. Ryu, R.P. Souto, P.F. Pilch, and C.Y. Jung. 1999. Separation and partial characterization of three distinct intracellular GLUT4 compartments in rat adipocytes. Subcellular fractionation without homogenization. *J. Biol. Chem.* 274:37755–37762.

Malide, D., N.K. Dwyer, E.J. Blanchette-Mackie, and S.W. Cushman. 1997. Immunocytochemical evidence that GLUT4 resides in a specialized translocation post-endosomal VAMP2-positive compartment in rat adipose cells in the absence of insulin. *J. Histochem. Cytochem.* 45:1083–1096.

Malide, D., G. Ramm, S.W. Cushman, and J.W. Slot. 2000. Immunoelectron microscopic evidence that GLUT4 translocation explains the stimulation of glucose transport in isolated rat white adipose cells. *J. Cell Sci.* 113:4203–4210.

Soumpasis, D.M. 1983. Theoretical analysis of fluorescence photobleaching recovery. *Biophys. J.* 41:95–97.